

Visualization of the role of the gas-water interface on the fate and transport of colloids in porous media

Jiamin Wan¹ and John L. Wilson

Department of Geoscience, New Mexico Institute of Technology, Socorro

Abstract. This paper exposes the significant role played by the gas-water interface in the fate and transport of colloids in porous media and also introduces a micromodel method to allow direct visualization of colloid behavior in pore networks. The gas-water interface was created by trapping air in the pore space. Various types of latex and clay particles, as well as bacteria, were studied. The results suggest that the gas-water interface sorbs not only hydrophobic but also hydrophilic particles. The degree of sorption is controlled by particle surface hydrophobicity, solution ionic strength, and particle charge sign. Sorption increases with increasing particle hydrophobicity and solution ionic strength, while positively charged particles have a very strong affinity for the gas-water interface. The sorption on the gas-water interface is essentially irreversible, in that the capillary free energy provides a large attractive force to hold particles on the gas-water interface after its rupture. These findings reveal a mechanism of vadose zone transport: A static gas-water interface behaves as a sorbent phase retarding the transport of particulate contaminants. The visualization method developed in this research is very useful for the investigation of particulate contaminant behavior and interface-related transport, especially in the context of bioremediation.

Introduction

Colloids are typically considered to be particles that range in size from 1 nm to 10 μm , including mineral fines, organic macromolecules, bacteria, viruses, etc. Organic and inorganic pollutants adsorb onto mobile colloids in the subsurface environment, thereby enhancing pollutant mobility [McDowell-Boyer *et al.*, 1986; Buddemeier and Hunt, 1988; McCarthy and Zachara, 1989; Gschwend, 1992]. In addition, some colloids are themselves toxic or virulent (i.e., bacteria and viruses). Colloid transport is concerned with colloid movement and sorption to and desorption from solid surfaces in porous aquifer media. In order to avoid specifying mechanisms, we chose the general and somewhat vague term "sorption" to describe the adhesion or attachment of colloids onto any interface. Historically, research on transport has focused on water-saturated porous media, but there are often other fluid phases present. Gas is one of the major fluid phases in the subsurface. In the vadose zone a continuous gas phase shares pore space with the aqueous phase. In the saturated zone, gas bubbles may be generated by various processes: entrapment of air as the water table fluctuates, organic and biogenic activities, or the emergence of gas from solution as the aqueous phase pressure drops, etc. In a common three-phase system of solid, water, and gas, with a water-wet solid surface, we have two principal interfaces: solid-water and gas-water. Although the solid-water interface has been extensively studied, the gas-water interface has been neglected. In this paper we present a study of the

role of this interface using a visualization tool, the etched glass micromodel.

Interactions of fine-grained minerals and gas bubbles have been extensively studied in the field of froth flotation [Laskowski, 1974; Derjaguin *et al.*, 1984; Fuerstenau, 1980; Leja, 1982; Hornaby and Leja, 1983; Jameson, 1985]. In froth flotation, valuable metals are separated from gangue minerals by selective sorption to gas bubbles running up through a mineral-surfactant-water slurry. The important differences between the present research and the flotation process are as follows: (1) The mineral particles in a flotation process are macroscopic particles compared to the microscopic colloids in a groundwater system. (2) In flotation the mineral particle surfaces are treated with the specific surfactants that impart a hydrophobic character to the desired particles. The surfaces of the bubbles are stabilized by adding surfactants. Natural porous media systems are essentially free of surfactant. (3) Flotation applications occur in a reactor vessel, whereas our study concerns porous media. The similarity between the two processes is in the surface forces that control the adhesion when particles and bubbles approach each other. These forces are also universal for any interacting surfaces in a liquid phase. They are electrostatic, van der Waals, and solvation forces [Israelachvili, 1991; Derjaguin *et al.*, 1987; Hirasaki, 1991].

Experimental Method and Materials

Glass Micromodels

Glass micromodels are created by etching a pore network pattern onto two glass plates which are then fused together in a furnace [Chatzis, 1982; Wilson *et al.*, 1990; Buckley, 1991; Conrad *et al.*, 1992]. Micromodel transparency allows microscopic investigation of fluid flow in a pore network composed of pore bodies connected by pore throats. Al-

¹Now at Lawrence Berkeley Laboratory, Berkeley, California.

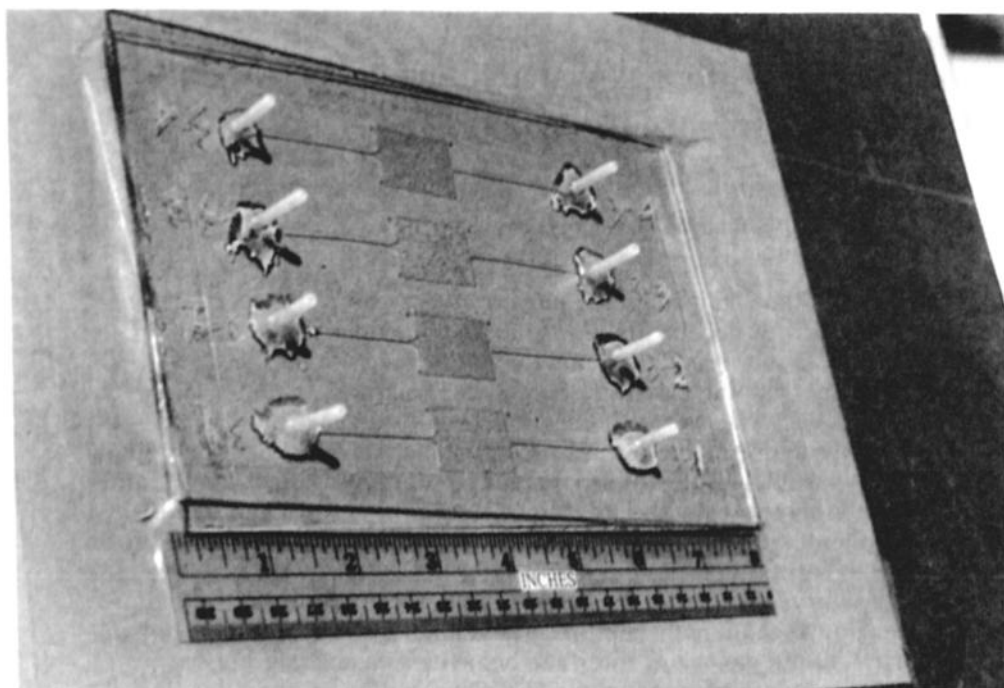


Figure 1. A glass micromodel plate containing four micromodels with heterogeneous networks. (1 inch equals 2.54 cm.)

though the network is only two-dimensional, the pores have a complex three-dimensional structure. Pore wedges, composed of corners of the pore bodies and throats where the glass plates meet, are a feature of the third dimension. The glass used for making micromodels has a chemical composition of 72% SiO_2 , 14% Na_2O , 3.8% CaO , and other trace metal oxides. In the presence of water, glass is covered with surface hydroxyl groups; the glass-water interface is negatively charged at neutral pH. The surface energy of glass is very similar to that of bulk aquifer solids. Thus the glass surface plays the role of the solid surface. Conventional micromodels have pore sizes varying from 0.1 to a few millimeters. The smaller pores are the more difficult to fabricate. Previous techniques were modified in this research. Pore sizes were reduced to a few micrometers, and four similar micromodels were fabricated in one glass plate at a time as illustrated in Figure 1. Micromodels were not reused in this research because of the difficulties of removing all of the attached particles while preserving a homogeneous surface chemistry. The pore volume in these micromodels was about 0.1–0.2 mL, measured by water weight. The pore network covered an area of about 3 cm^2 . Micromodels with three different pore network patterns were generated, and Figure 2 shows their microphotographs taken from actual micromodel networks. Figure 2a shows a portion of a homogeneous quadrilateral network having 1225 pore bodies. An air bubble is trapped in each of the pore bodies in this photo. Pore bodies and pore throats are sized at about $200 \mu\text{m}$ and $50 \mu\text{m}$ in diameter, respectively. Figure 2b shows part of a homogeneous hexagonal network having 1116 pore bodies in each model. Pore bodies and throats are sized $300 \mu\text{m}$ and $20\text{--}100 \mu\text{m}$, respectively, in diameter. Figure 2c has a heterogeneous network with preferential flow paths. Pore sizes vary from 4 to $400 \mu\text{m}$ in diameter. This paper focuses on effects of surface chemistry, and most of the experiments

in this research were carried out in quadrilateral networks. Although the influence of pore configuration is not discussed in this paper, these photos show the potential of using this technique to study the effect of fluid dynamics on colloid collision efficiency, and other related subjects.

Colloidal Particles

Fluorescent latex microspheres (Interfacial Dynamics Company) were used as model particles in this research because they were easy to observe, had well-defined physical-chemical characteristics, and were manufactured without surfactant. The yellow-green fluorospheres we chose can be more efficiently illuminated than other color types. According to the manufacturer's report, the fluorescent dyes have no significant effect on the surface properties of the latex particles. Clay and bacteria were also tested because of their importance in groundwater. The six types of particles and their size and surface characteristics are listed in Table 1: (1) Hydrophilic, negatively charged latex: These high-surface charge density, hydrophilic latexes are manufactured from hydrophobic sulfate charge-stabilized latexes. The process consists of grafting carboxylic acid polymers to the particle surface to produce a porous, highly charged surface layer. The final functional surface groups are predominantly carboxylate with an insignificant amount of sulfate. (2) Hydrophobic, negatively charged latex: These microspheres are also stabilized by sulfate charges, but the surface functional groups are sulfate and hydroxylate. Their hydrophobicity is attributed to low charge density. (3) Positively charged, hydrophobic latex: The only surface functional group present on these particles is amidine. The surface charge density is relatively low, and the particles have a hydrophobic surface. According to manufacturer's report these latex particle suspensions are surfactant-free. We used the purchased products without further cleaning.

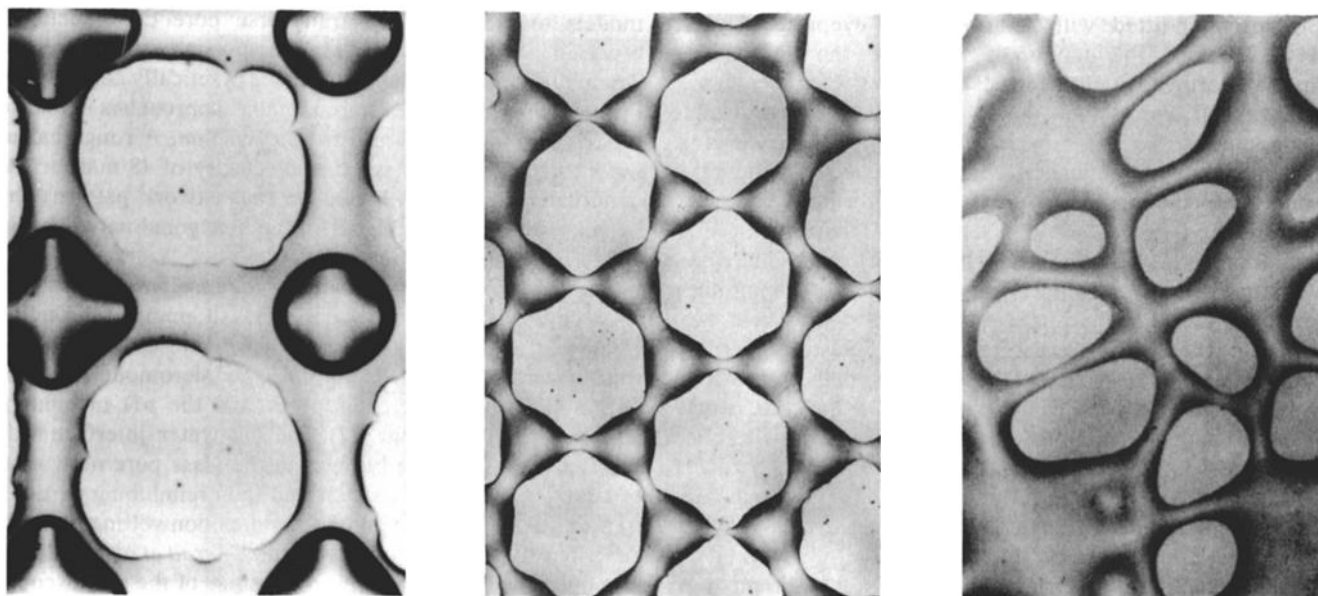


Figure 2. Three pore networks used in this study: (a) quadrilateral network; (b) hexagonal network; (c) heterogeneous network.

(4) Na-montmorillonite (Source Clay, Columbia, Mississippi): Particles were sorted with a centrifuge, and particle size was measured with a scanning electron microscope. To diminish the influence of organics, the clay particles were washed with a series of solvents in the order of chloroform-methanol-water. (5) Hydrophilic bacteria: *Pseudomonas cepacia* 3N3A was isolated by Brockman *et al.* [1989] from sediment samples from a depth of 203 m near Aiken, South Carolina. (6) Relatively hydrophobic bacteria: *Arthrobacter sp.* S-139 was isolated by Aaron Mills and others from a shallow groundwater aquifer. Bacteria sizes were measured with an optical microscope. Both strains were grown in 10% PTYG broth at 27°C on a shaker (200 rpm). When the culture reached a late logarithmic stage of growth (36–48 hours), cells were harvested by centrifugation (5000 × *g* for 10 min) and washed three times in a sterile solution of 1.0 mM NaNO₃ at pH 6.6. Cells were then suspended in the same solution. The concentrated suspension was stored by refrigeration.

Characterization of Particle Surface Hydrophobicity

Particle electrophoretic mobility is an indirect measurement of particle surface hydrophobicity. The measurements of electrophoretic mobility were conducted in a solution of 1.0 mM NaNO₃ and pH 6.6 at 25°C (see Table 1). Analyses

were carried out in a Coulter DELSA 440 (Doppler electrophoretic light scattering analyzer). The instrument monitors the light scattered from the moving particles at four angles. The reported mean was computed from these four analyses.

Contact angle is a relative measurement of the hydrophobicity of the surface which in most cases shows a correlation with the surface free energy. We modified a technique to measure surface contact angles of all particles presented in this paper by using a thin particle layer in a classic captive drop method [Gaudin *et al.*, 1963]. Particle layers for contact angle measurements were prepared with two methods, filtering and smearing. There was no significant difference in the results from the two methods. In the filtering method a high-concentration particle suspension was filtered through a 0.45- μm pore size micropore filter. The filter, with a 50–100 μm thickness of packed particles, was fixed on a glass slide. The slide was allowed to dry in a desiccator until the particle layer began to crack (it took about 2 hours). The smearing method was used for very fine particles including clay and fine latex particles ($\leq 0.45 \mu\text{m}$) because they were difficult to filter. A highly concentrated particle suspension was smeared on a clean glass slide to a thickness of 50–100 μm . The smearing slide took about 3–4 hours to dry. Contact angles were measured directly with a microscope (Carl Zeiss

Table 1. Particles Used in Micromodel Experiments

Descriptive Term	Particle Types	Size, μm	Electrophoretic Mobility, $\mu\text{m s}^{-1} \text{v}^{-1} \text{cm}^{-1}$	Contact Angle θ_a
Hydrophilic, negatively charged latex	carboxylate latex	0.95	-7.1 ± 0.2	$<10^\circ$
Hydrophobic, negatively charged latex	sulfate latex	1.05	-3.8 ± 0.2	$127 \pm 7^\circ$
Hydrophobic, positively charged latex	amidine latex	0.60	$+5.0 \pm 0.3$	$109 \pm 5^\circ$
Clay	Na-montmorillonite	~ 0.5	-2.9 ± 0.1	$37 \pm 3^\circ$
Hydrophilic bacteria	bacteria 3N3A	1.2×0.8	-1.0 ± 0.3	$25 \pm 3^\circ$
Hydrophobic bacteria	bacteria S-139	1.0×0.8	-4.5 ± 0.4	$77 \pm 3^\circ$

Stereoscope) fitted with a goniometer eyepiece (Eyocla 4443, Tokyo) at the junction of the drop of the solution, the layer of particles, and the atmosphere at 24°C. The solution was 1.0 mM NaNO₃ with pH 6.6. The initial water advancing contact angles are reported in Table 1. The readings of the initial advancing angles were taken about 2 s after the water drop contacted the surface. Each reported contact angle is the mean of ≥ 15 measurements. There are several limitations with this method. The contact angle decreases with time because the "porous medium" of packed particles imbibes water. The measured value depends on particle size, layer thickness, layer moisture content, and the recording time for the contact angle. Therefore this method measures only relative surface hydrophobicities under the same experimental conditions for the same category of particles. For example, do not compare contact angles of latex particles with bacteria to determine which one is more hydrophobic. Also do not attempt to calculate particle surface free energy from these contact angle values.

In general, electrophoretic mobility is a measurement of particle surface charge for particles having same size and density in the same solution. Surface charge density is related to surface hydrophobicity but does not determine it. There is a general trend for similar nonbiogenic particles: The greater the electrophoretic mobility, the lower the surface hydrophobicity, and the smaller the water contact angle. In Table 1 this relationship is shown by the data for latex particles. Data for bacteria show an opposite correlation, that is, water contact angle increases with the increasing electrophoretic mobility. Van Loonrecht *et al.* [1987] reported the same correlation for bacteria.

Experimental Procedure

A high-resolution optical microscope (Zeiss AxioPhot) with fluorescent lighting, dark field image and long working distance objectives was used. During experiments a prepared micromodel was mounted horizontally on the stage of the microscope. Flow rate was precisely controlled by a syringe pump (Harvard Apparatus, model 4400-001). Photomicrographs and a video recording were taken simultaneously.

In order to simulate groundwater conditions, the solution chemistry was designed conservatively with exceptions noted later. The ionic strength of the solutions and suspensions was 1.0 mM NaNO₃. A pH of 6.6 was maintained by NaHCO₃ in all the solutions and suspensions. Air was used as the gas phase. All chemicals used were prepared using distilled and deionized water. Degassed solution was made by using degassed-distilled-deionized water and maintained on a vacuum line before use. Particle number concentration was about 5×10^7 mL⁻¹ for all of the suspensions except the clay which is unknown. To simulate groundwater conditions, the flow velocity was designed to be relatively low, but was experimentally limited by the small pore volume of the micromodels. Constant volume flow rate of 1.5 mL/h was maintained with exceptions noted later. The average linear velocity in the micromodels is unknown. Had it been available, particle velocimetry could have been used to directly calculate this parameter. But this technology has never been applied to a micromodel. An indirect calculation using the volumetric flow rate requires an estimate of porosity and other geometric factors, which have a different interpretation in two-dimensional networks, or destruction of the

models to measure their transverse pore cross-sectional area. The indirect approach also requires an estimation of in situ fluid saturation, which cannot be practically achieved by the standard volumetric or gravimetric approaches in micromodels with only 0.15 mL of pore volume. A rough calculation suggests an average linear velocity of 48 m/d for the quadrilateral network. Based on the network patterns the velocity was probably higher in the hexagonal network and lowest in the random network.

The visualization experiment procedure was as follows: (1) A degassed solution was continuously pumped through a clean micromodel at a relatively high rate of 15 mL/h to saturate and chemically equilibrate the micromodel, until all of the air bubbles were dissolved and the pH of effluent equaled that of influent. (2) The gas-water interface was created, as residual air bubbles in the glass pore networks, by draining the model with air and then reimbibing particle-free solution. The concept of a residual nonwetting phase is described by Wilson *et al.* [1990] and Conrad *et al.* [1992]. (3) The micromodel was placed on the stage of the microscope. A dilute particle suspension was injected at a constant rate (1.5 mL/h) for 30 pore volumes. Particle behavior was observed and recorded. (4) The particle suspension was replaced with a particle-free solution at the same flow rate until all free particles were displaced, leaving only particles attached on interfaces. All of the photos presented later, showing sorbed particles, were taken after this step. Therefore the comparisons of results were based on the same experiment conditions.

Experimental Results and Discussion

Gas-Water Interface and Hydrophilic Particles

Although classical criteria separating hydrophilic and hydrophobic surfaces involve a water contact angle that is less or greater than some reference angle (usually 0° or 90° depending on the preference), this study refers, instead, to relative hydrophilicity and hydrophobicity. We classify particles with low water contact angle as relatively hydrophilic particles and those with greater contact angle as relatively hydrophobic particles. For instance, we believe that most of the naturally generated abundant inorganic colloids, such as fines of clay, silica, and the other metal oxides, are relatively hydrophilic.

Within the framework of the DLVO theory the sum of the van der Waals and electrical double layer interaction forces forms the total energy of interaction [Derjaguin and Landau, 1941; Verwey and Overbeek, 1948]. Knowing solution ionic strength 1.0 mM, particle zeta potential -90 mV (from measured electrophoretic mobility), and assuming zeta potential of glass surface -60 mV [Elimelech and O'Melia, 1990], and zeta potential of gas bubble -40 mV [Lee and McCammon, 1984; Yoon and Yordan, 1986; Li and Somasundaran, 1991], we calculated two pairs of interaction potentials: those involving a negatively charged, hydrophilic particle with a negatively charged, hydrophilic glass surface and the same particle with a gas bubble. For the hydrophilic particle-glass pair, the absolute value of repulsive electrostatic potential is greater than the attractive van der Waals potential; thus the net interaction potential is repulsive. (We neglect the repulsive hydration potential between two hydrophilic surfaces.) For the hydrophilic particle-gas bubble pair the electrostatic force is repulsive, and van der Waals

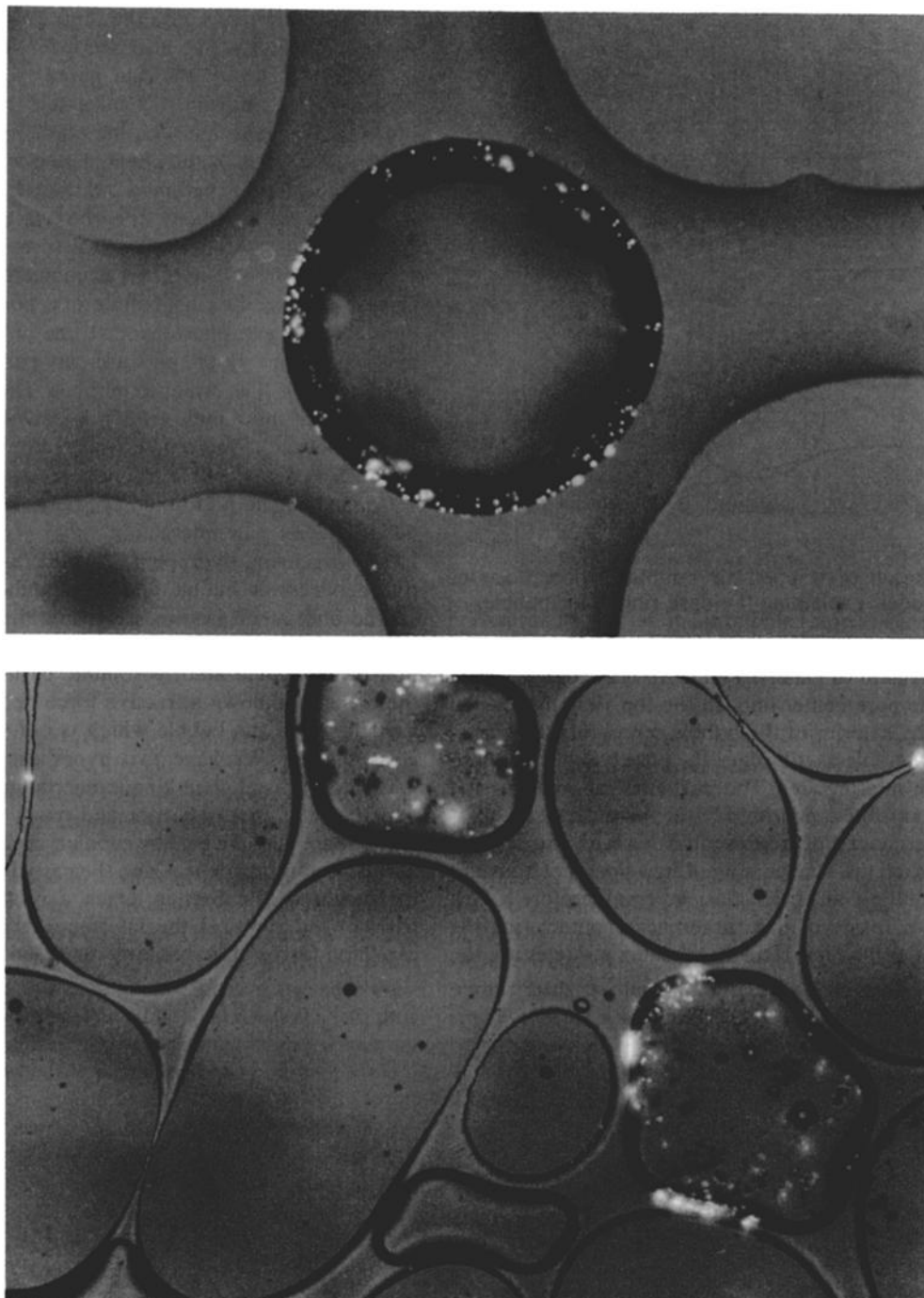


Plate 1. Hydrophilic negatively charged latex particles ($0.95 \mu\text{m}$) preferentially sorbed onto air bubbles versus pore walls: (a) air bubble trapped in pore body of quadrilateral network; (b) air bubbles trapped in heterogeneous network. Some fine pore throats physically plugged by particles.

force is also repulsive due to the positive complex Hamaker constant [Hamaker, 1937; Van Oss *et al.*, 1983; Li and Somasundaran, 1991]. Hence the net interaction energy is repulsive. Therefore, according to DLVO theory, the hydrophilic particles used in this research should not sorb onto either the glass-water or the gas-water interfaces.

Fluorescent carboxyl latex (diameter, $0.95 \mu\text{m}$; $\theta_a < 10^\circ$), Na-montmorillonite (diameter, $0.5 \mu\text{m}$; $\theta_a = 37^\circ$) and bacteria 3N3A ($1.2 \times 0.8 \mu\text{m}$, $\theta_a = 25^\circ$) were used to test

the behavior of hydrophilic particles at interfaces. The visualized phenomena were recorded photographically and on videotape. In Plate 1a a single air bubble is trapped in a pore body of a quadrilateral network, and in Plate 1b a few bubbles are trapped in a heterogeneous network. Both pictures show that hydrophilic latex particles preferentially sorb onto the air-water interface but very few particles attach to the pore walls. Figure 3 is a sketch of an air bubble trapped in a pore body of a glass micromodel. Figure 3a is a

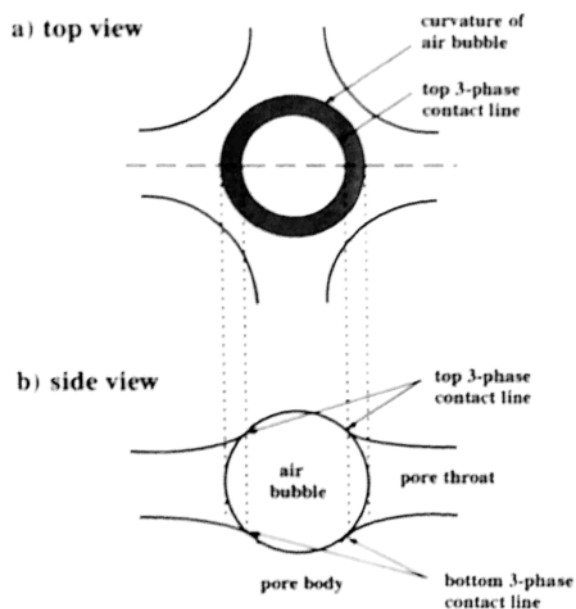


Figure 3. Sketch of trapped air bubble in pore body of glass micromodel, explaining the dark ring of air bubble

top view equivalent to Plate 1. Figure 3b is a cross sectional view along the pore center line. In the top view the shaded ring around the exterior of the bubble represents the curvature of the air bubble as it bridges the pore body from top to bottom of the micromodel. The curvature approaches the top and bottom of the micromodel at the three phase (air-water-glass) contact line represented here as the interior circumference of the shaded ring. Light does not transmit through the multiple air-water-glass layers, therefore a dark ring is formed. Inside of this three-phase contact ring the water phase is a thin film. Usually the latex particles are too

big to enter this film, but we see some particles in Plate 1b have found their way into the film. This may be caused by surface roughness. We also see a few particles have been strained by some of the fine pores, perhaps plugging the throats. The behavior of hydrophilic particles on the air bubbles is inconsistent with the prediction based on DLVO theory. This unexpected phenomenon was also found in the clay and bacteria experiments. If there is any question about the surface hydrophilicity of carboxylate latex particles, the sorption of clay particles is a real surprise. Figure 4 shows Na-montmorillonite particles accumulated onto the downstream portion of an air bubble in a pore body. The lower curve is the three-phase contact line of top glass plate, air, and water. The white spots are clay particles that accumulated near this line, which is in focus. The upper curve is the curvature of the bubble, which is between two glass plates and unfocused. Figure 5 shows hydrophilic bacteria accumulated on a gas bubble trapped in a pore body.

Comparing the partitioning of particles on the two interfaces, the net pair interaction energy is repulsive between glass surface and hydrophilic particle, and relatively attractive between air bubble and hydrophilic particle. The observed bulk result is consistent with the prediction for the pair of glass and hydrophilic particle, but inconsistent for that of air bubble and hydrophilic particle. It is clear that there is an unknown attractive force between a hydrophilic particle and a gas bubble which is not associated with the glass surface. We have two hypotheses. The first is that particles with sufficient kinetic energy imparted by the flow penetrate the energy barrier and reach the air-water interface, where they are held by capillary forces. The probability of this penetration depends on the particle kinetic energy and the height of the barrier. Once a particle penetrates the barrier, and ruptures the interface, it will be retained by capillary forces if it has any finite contact angle, as we

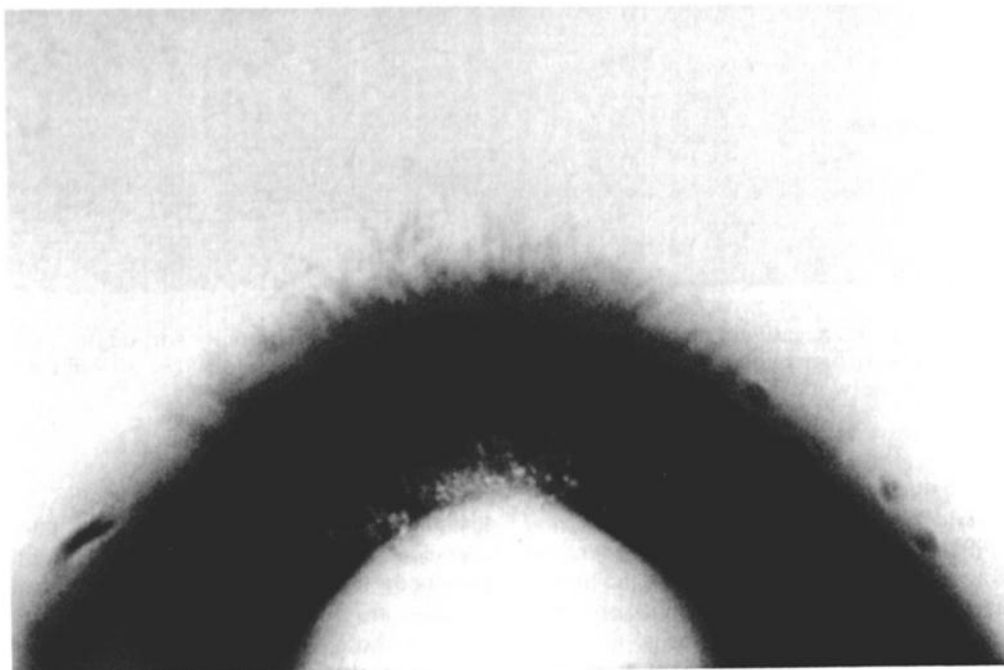


Figure 4. Na-montmorillonite particles ($\sim 0.5 \mu\text{m}$) accumulated on downstream side of air bubble trapped in pore body of hexagonal network. Air bubble is about $300 \mu\text{m}$ in diameter.

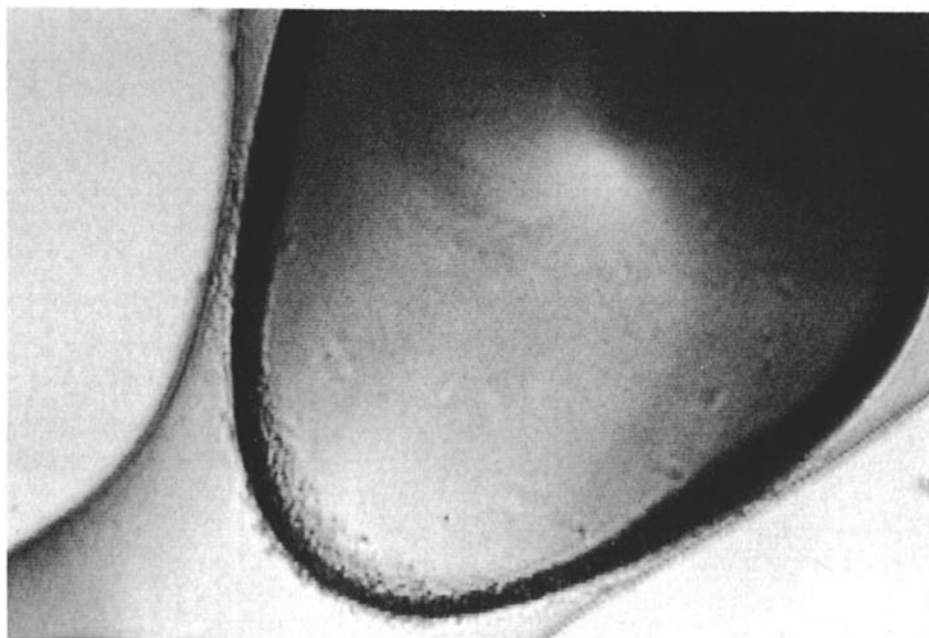


Figure 5. Hydrophilic bacteria 3N3A ($1.3 \times 0.8 \mu\text{m}$) preferentially sorbed on air bubble trapped in a pore body of the hexagonal network.

describe for desorption below. The second hypothesis is that the hydration force between the gas bubble and hydrophilic particle is attractive. DLVO theory cannot explain all the known facts about the stability of colloids and thin liquid films. The discrepancies are ascribed to "solvation" of the surfaces. Solvation implies formation of boundary layers of special molecular structure, different from that of the bulk liquid. The first shell of water molecules around a particle surface is usually referred to as the primary hydration shell. This is where the water molecules are most restricted in their motion. The effect propagates out beyond the first shell; thus in the second hydration shell the water molecules are somewhat free to rotate and exchange with bulk water; in the third shell they are even more so, extending a few molecular diameters. This region of modified solvent structure is referred to as the solvation zone. When the solvation zones of two surfaces overlap, a short-range force arises that is now usually referred to as a solvation or structure force and, when water is the solvent, hydration force [Israelachvili, 1991]. The orientation and density of water molecules in the hydration zone are important in determining the overall hydration force. Understanding of the water molecular structure at the gas-water interface is still in its infancy. Gas is nonpolar and hydrophobic. Water density at the gas-water interface is lower than bulk water density. There is an attractive interaction between water molecules and a hydrophilic surface, and thus water density at a hydrophilic surface is higher than the bulk density. A repulsive force arises when the density of water between the two surfaces increases as they approach each other, while an attractive interaction arises if the density falls, that is, if the region between the two surfaces becomes depleted of water. For two sufficiently hydrophobic surfaces the latter should result in the attraction of the two surfaces toward each other [Christenson and Claesson, 1988]. The degree of the hydration force between a gas bubble and a hydrophilic particle

should lie somewhere in between that for two hydrophilic surfaces and for two hydrophobic surfaces.

Sorption and Particle Surface Hydrophobicity

Colloids in the subsurface environment have a wide range of surface wettability. Various types of natural and man-made organic colloids are hydrophobic. Also, the adsorption of organic matter onto hydrophilic particles can alter their surface wettability. Plate 2 shows the distribution of hydrophobic latex particles (diameter, $1.05 \mu\text{m}$; $\theta_a = 127^\circ$) in a single pore with a trapped air bubble. In comparing sorptive behavior as a function of hydrophobicity (all the other experimental conditions are the same), we see many more hydrophobic latex particles sorbed onto both the air bubble and the pore walls (Plate 2) than we saw earlier with hydrophilic ones (Plate 1). Hydrophobic latex particles show a greater affinity to both air-water and glass-water interfaces because, first, a hydrophobic surface of a latex particle has lower charge density than a hydrophilic one does and therefore the electrostatic repulsive force is lower. Second, the hydration force for hydrophobic particles is relatively more attractive than for hydrophilic ones. This phenomenon is also shown by the bacteria experiments. In Figure 6 the relatively hydrophobic bacteria S-139 ($1.0 \times 0.8 \mu\text{m}$; $\theta_a = 77^\circ$) greatly prefer the gas-water interface. In addition, many more bacteria sorbed onto the glass surface relative to the hydrophilic bacteria in Figure 5. Comparing the sorption of latex particles and bacteria on the gas-water interface, we notice that many bacteria appear to have crossed the three-phase contact line and entered into the apparent two-phase contact area of glass and air (where there is a thin water film).

Sorption and Particle Surface Charge Sign

A suspension of positively charged latex particles (diameter, $0.60 \mu\text{m}$; $\theta_a = 109^\circ$) was pumped through the micro-

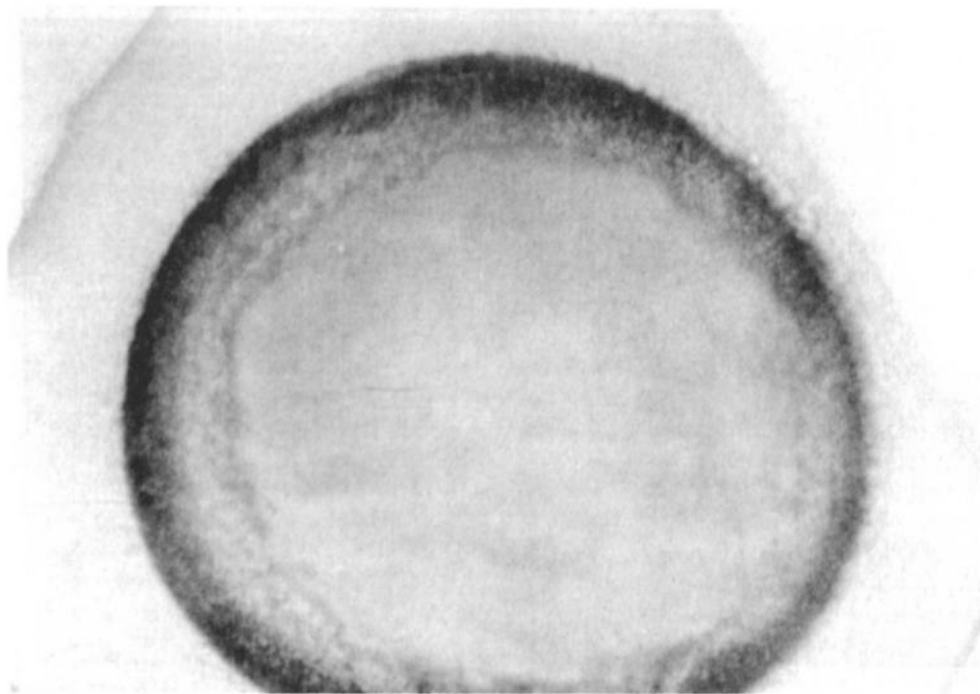


Figure 6. Relatively hydrophobic bacteria S 139 ($1.0 \pm 0.8 \mu\text{m}$) accumulated on air bubble in pore body of hexagonal network

models using the same experimental procedure. Plate 3 shows an entire air bubble and the adjacent glass surface covered by sorbed particles. Both interfaces have a higher affinity for positively charged hydrophobic particles rather than for the negatively charged hydrophobic particles shown earlier in Plate 2. Those particles were more hydrophobic ($\theta_w = 127^\circ$), and larger ($1.05 \mu\text{m}$). In Plate 3 the focus is on the top three phase contact line and the curvature is slightly off focus, but we can see that the whole boundary area is solid with the sorbed particles. The increased sorption of particles on the glass surface is due to the attractive electrostatic force between the oppositely charged particle and glass surfaces. The increased sorption on the gas-water interface is also caused by an attractive electrostatic force. We believe that the negative polarity of bubble surface is due to water molecule reorientation. Several researchers have reported, in the floatation literature, negative values for electrostatic mobility [Lee and McCammon, 1984; Yoon and Jordan, 1986; Li and Somasundaram, 1991].

Sorption and Solution Ionic Strength

Sorption in solutions of different ionic strength was tested with hydrophilic negatively charged latex (diameter, $0.95 \mu\text{m}$; $\theta_w = 10^\circ$). The results shown in Plate 4 indicate that with increasing solution ionic strength, there is increasing sorption on both trapped bubbles and pore walls. In a 1.0 mM solution (Plate 4a), particles sorb only on the gas bubbles. In Plate 4b, ionic strength is increased by a factor of 100, and sorption increases on both bubbles and pore walls due to double layer compression; thus sorption onto the gas-water interface increases with increasing solution ionic strength.

Desorption

Examination of particle desorption helps to reveal the energy status of interfaces and the sorption mechanism. In

these experiments we tested desorption from interfaces by decreasing ionic strength and by increasing flow rate, using hydrophilic negatively charged latex particles (diameter, $0.95 \mu\text{m}$; $\theta_w = 10^\circ$). In the first step, 30 pore volumes of particle suspension with high ionic strength (100.0 mM) was flushed through a prepared micromodel at 1.5 mL/h ; then a particle free solution with the same ionic strength (100.0 mM) displaced the particle suspension at the same flow rate. In Plate 5a we see that a high population of particles was sorbed onto both the glass and the residual air bubbles. After this, distilled and deionized (D-D) water was injected at the same flow rate in order to facilitate desorption behavior in a solution of decreasing ionic strength. As recorded on videotapes we observed desorption from glass pore walls, but none from the gas bubbles. Some of these desorbed particles were later captured by downstream gas bubbles as the particles passed by. Plate 5b was taken after 30 pore volumes of D-D water had flowed through the model. Most of the particles attached on the glass have been removed, and the number of particles on the gas bubbles has increased. In other experiments, where we increased flow rate 10 times (15 mL/h) rather than changed ionic strength, the result was almost the same. These experiments indicate that the attractive force is larger at the gas-water interface than at the solid-water interface for the same particles under the same chemical conditions and that sorption on the gas-water interface is essentially irreversible.

In the context of a general interaction potential isotherm [Hirasaki, 1991], irreversibility indicates that the sorption may occur in the primary minimum and the particles must have overcome the energy barrier. A question arises, What is the high adhesion energy between particles and air bubbles? We suggest capillary energy, based on the work done by James [1974], Rapacchietta and Neumann [1977], and Williams and Berg [1992]. If by any means the nonwetting

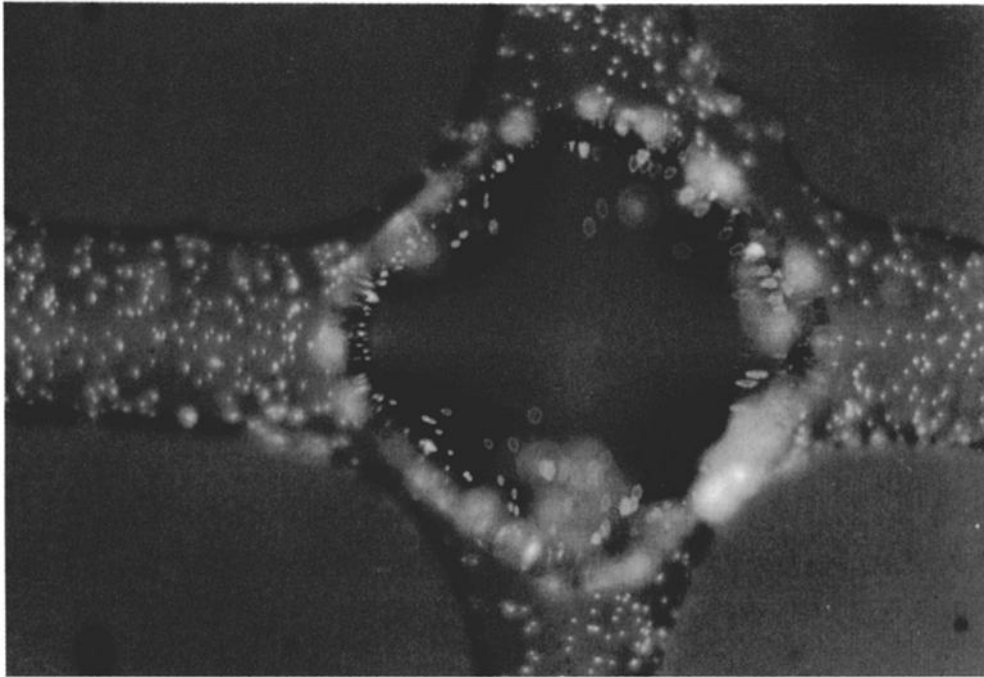


Plate 2. Hydrophobic negatively charged latex particles sorbed on both air-water and glass-water interfaces; air bubble is trapped in pore body of quadrilateral network. Observe the effect of particle surface hydrophobicity by comparing to Plate 1.

particles (contact angle >0) can overcome the energy barrier created by the superposition of the van der Waals force, the electrostatic force, and the hydration force, their surfaces will contact the interface and a three-phase contact line (gas, water, particle) will be formed on the particle surface. The capillary force, developed as soon as the three-phase contact line is established, will fix the particle at an equilibrium

position at the interface. The exact calculation of such a force involves solving a nonlinear ordinary differential equation for the meniscus profiles and is only possible for the simplest geometry. A comprehensive treatment of capillary force was given by *Rapacchietta and Neumann* [1977]. In their work, both force and free energy were analyzed to determine the particle's equilibrium position at the interface.

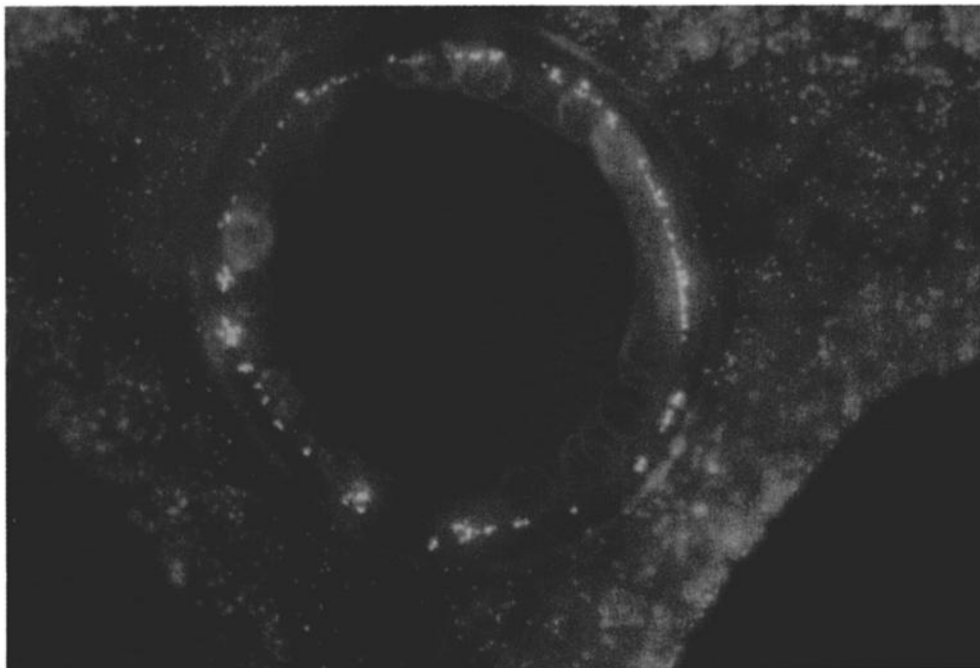


Plate 3. Positively charged hydrophobic latex particles ($0.6 \mu\text{m}$) with very strong affinity for both gas-water and glass-water interfaces. Hexagonal network.

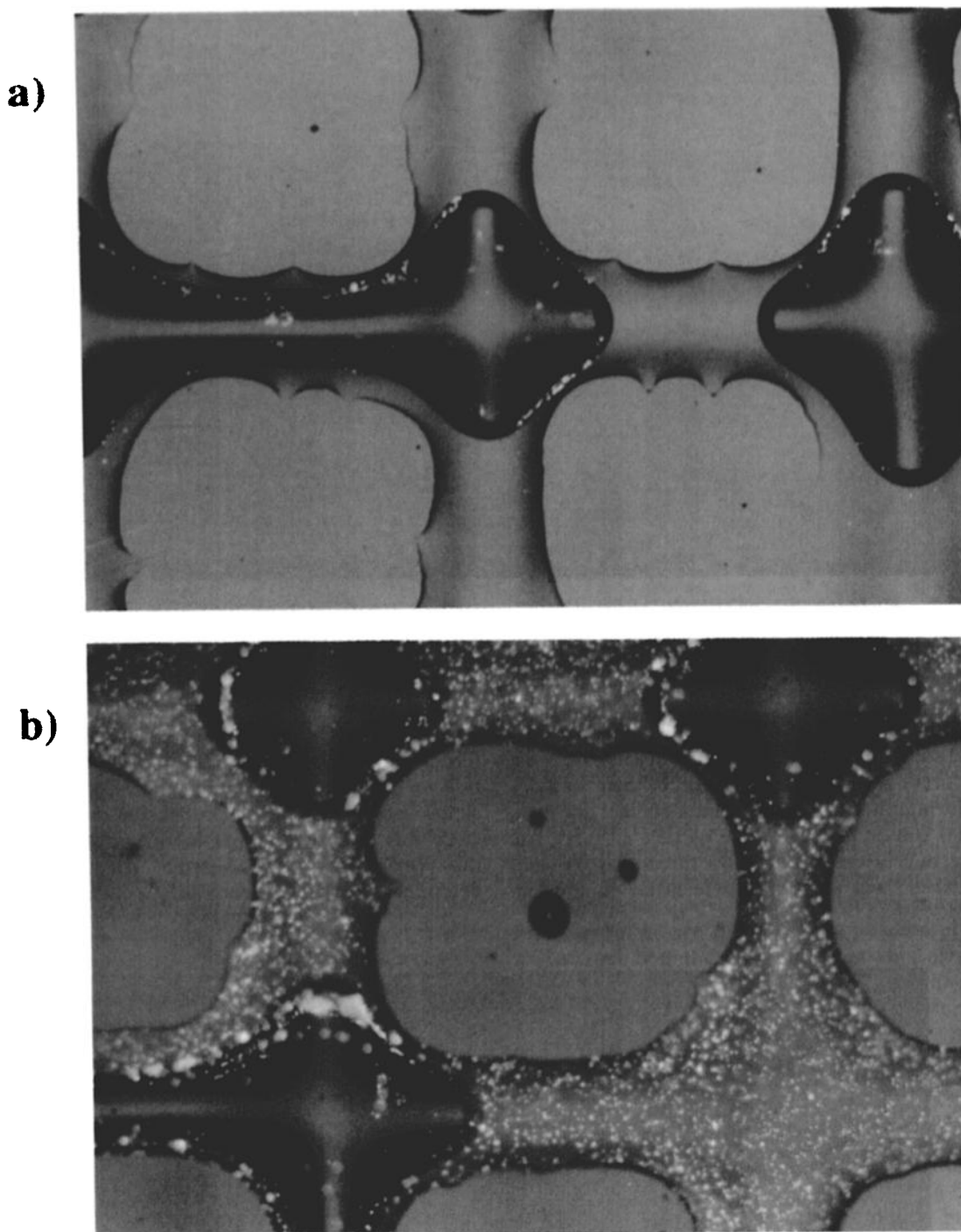


Plate 4. The effect of solution ionic strength on sorption: (a) In low ionic strength (1.0 mM) solution, hydrophilic latex particles only sorb on gas-water interface. (b) Ionic strength is increased by a factor of 100; many more particles sorb on both bubbles and pore walls. The experiment was carried out in a quadrilateral network.

These calculations are quite complicated. However, the problem can be significantly simplified in the case of particles of colloidal size, where the effect of gravitational force can be ignored when compared to the surface tension, and the meniscus can be approximated as a flat one. This asymptotic behavior was checked by examining the James matched asymptotic expansion [James, 1974; Williams and Berg, 1992] for the meniscus profile about a small circular

meniscus and using it to calculate the particle position with the model of Rapacchietta and Neumann. This simplified analysis is schematically described in Figure 7. Consider a particle (radius equal to r), which is fully immersed in a liquid with initial wetted semicircle $\phi = \pi$, that passes through the gas-water interface and becomes partially immersed ($\phi = \pi - \theta$, θ is contact angle). The free energy variation in this case is due to two contributions: the work (dE_1) required to

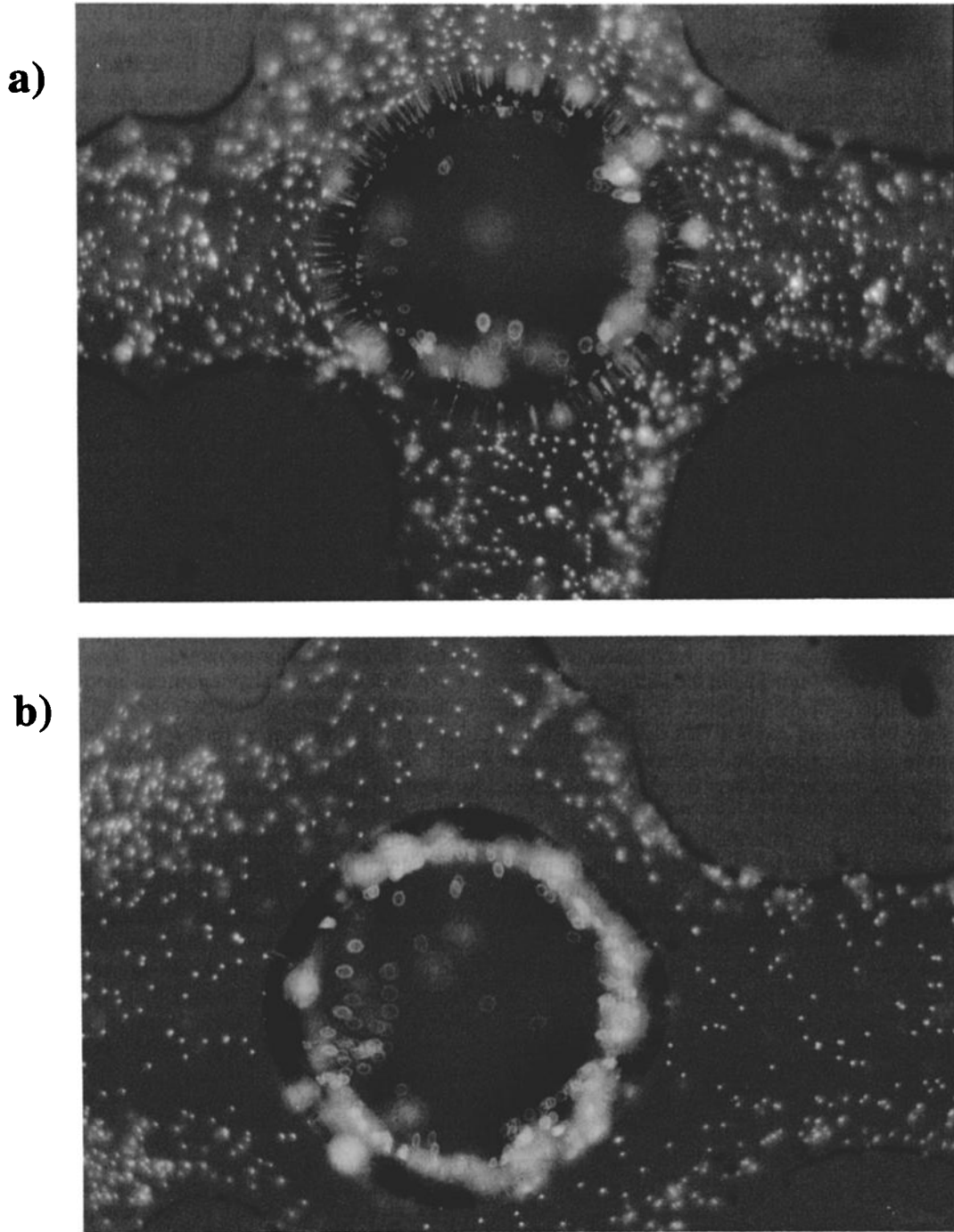


Plate 5. Desorption as solution ionic strength decreases: (a) in high ionic strength solution (100.0 mM) at 1.5 mL/h, showing hydrophilic latex particles that have sorbed onto the interfaces; (b) after the passage of 30 pore volumes of distilled and deionized water at same flow rate. Air bubble ($\sim 200 \mu\text{m}$ diameter) is trapped in pore body of quadrilateral network.

replace area A_{sg} of surface energy σ_{sl} with equivalent area of surface energy σ_{sg} and the work (dE_2) done by eliminating the gas-water interface.

$$\begin{aligned} dE_1 &= A_{sg}(\sigma_{sg} - \sigma_{sl}) = A_{sg}\sigma_{lg} \cos \theta \\ &= 2\pi r^2 \sigma_{lg}(1 + \cos \phi) \cos \theta \quad (1) \end{aligned}$$

$$dE_2 = -A_{lg}\sigma_{lg} = -\pi r^2 \sin^2 \phi \sigma_{lg} \quad (2)$$

The capillary potential E_{cap} , which is defined as the total free energy variation, can be expressed as

$$\begin{aligned} E_{\text{cap}} = dE_1 + dE_2 &= \pi r^2 \sigma_{lg} [2 \cos \theta (1 + \cos \phi) - \sin^2 \phi] \\ &= -\pi r^2 \sigma_{lg} (1 - \cos \theta)^2 \quad (3) \end{aligned}$$

Figure 8 shows the calculated result of the capillary free energy change as a function of the contact angle. In this

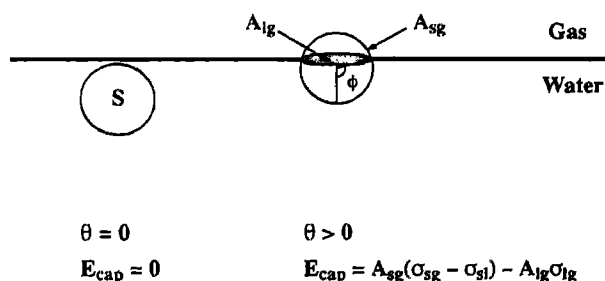


Figure 7. The capillary free energy change E_{cap} fixes the particles on the interface after the rupture of the interface. Here ϕ denotes wetted semiarc; θ , contact angle; A_{sg} , area of dewetted particle surface, function of contact angle; A_{lg} , area of gas-water interface displaced by particle, function of contact angle; σ_{sg} , particle-gas interface energy; σ_{sl} , particle-water interface energy; σ_{lg} , gas-water interface energy.

calculation the particle was assumed to be 1.0 μm in diameter and $\sigma_{\text{lg}} = 73$ dyn/cm. Capillary potential increases rapidly with the increasing of the contact angle.

Therefore we suggest that the sorption of particles onto the gas-water interface has two energy stages. The DLVO and hydration forces control the first stage, in which the interface is ruptured; and after the three-phase contact line is established, the capillary force fixes each particle at an equilibrium position on the interface in the second stage. The capillary force strongly binds particles on the gas-water interface, so they essentially cannot be desorbed from the gas-water interface. In fact, the entire bubble-particle unit can be moved by increasing the flow rate without particle desorption.

A subsidiary observation, especially apparent on videotapes of the experiments, was the rapid circulation of particles along the bubble surface in all of the micromodel experiments. Most of the circulation paths were localized on a bubble surface, and the speed was proportional to the flow rate. This is probably related to the interaction between the outside shear stress in the flowing water and the air movement inside the bubble. Particles also tended to accumulate on the downstream portions of bubbles at higher flow rates, in the stagnation zone located there. The particles sorbed on

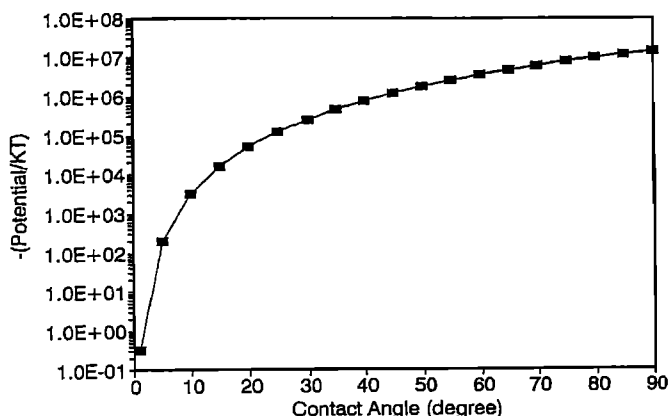


Figure 8. The calculated capillary free energy change as a function of contact angles for a 1- μm spherical particle near a large air bubble, normalized by KT , where K is Boltzmann's constant and T is absolute temperature.

the air bubbles also tended to form aggregates especially if they were hydrophobic (see Plates 1a, 2, 4, and 5). This tendency is presumably due to a capillary attraction between particles on the interface. It becomes stronger when the system is disturbed, for example, by increasing flow rate, changing flow direction, and especially by moving the bubbles. The videotape recordings dramatize the dynamic aspects of these phenomena.

Summary and Conclusions

We developed a method to visualize the behavior of colloid particles at interfaces within pore networks. Visualization was achieved by using glass micromodels with a UV epifluorescent light and dark field microscope. This method allowed direct observation of the interactions of colloids and interfaces both globally throughout the network and locally within individual pores. Besides fluorescent latex particles, common natural colloids, such as clay and bacteria, were directly observable. The wettability of the pore walls, the fluid phase distribution within the pore network, the flow rate, and the chemical conditions of the system could all be closely controlled. Thus the method reveals both cause and effect. This method can be used in future studies of particulate transport, interface-related transport, and the facilitation of bioremediation schemes.

We isolated several phenomena in our interface-related colloid transport study. The gas-water interface preferentially sorbs colloidal particles relative to the solid-water interface under simulated groundwater conditions. The degree of this sorption increases with increasing particle surface hydrophobicity and increasing solution ionic strength. Positively charged particles have greater affinity to the gas-water interface. The sorption at the gas-water interface is irreversible due to the capillary free energy change. Once sorbed onto the interface, few particles can be desorbed by chemistry or shear stress. The preferential sorption of colloid particles onto the gas-water interface suggests a mechanism in vadose zone transport. A stationary gas-water interface in porous media can retard the transport of particulate contaminants. Moving interfaces, such as during infiltration or drainage or near a fluctuating water table, may enhance colloid mobility.

Acknowledgments. The authors would like to acknowledge Norman Morrow, Robert Bowman, Jill Buckley, and Tom Kieft for their helpful discussions. We thank Robert TerBerg for help with editing this manuscript. We also would like to acknowledge the Subsurface Science Program, Office of Health and Environmental Research, U.S. Department of Energy for supporting this work under DOE grant DE-FG04-89ER60829.

References

- Brockman, F. J., B. A. Denovan, R. J. Hicks, and J. K. Fredrickson, Isolation and characterization of quinoline-degrading bacteria from subsurface sediments, *Appl. Environ. Microbiol.*, 55, 1029-1032, 1989.
- Buckley, J. S., Multiphase displacements in micromodels, in *Interfacial Phenomena in Petroleum Recovery*, edited by N. R. Morrow, pp. 157-189, Marcel Dekker, New York, 1991.
- Buddemeier, R. W., and J. R. Hunt, Transport of colloidal contaminants in groundwater: Radionuclide migration at the Nevada test site, *Appl. Geochem.*, 3, 535-548, 1988.
- Chatzis, I., Photofabrication technique of two-dimensional glass

- micromodels, *PRRC Rep. 82-12*, N. M. Inst. of Min. and Technol., Socorro, 1982.
- Christenson, H. K., and P. M. Claesson, Cavitation and the interaction between macroscopic hydrophobic surfaces, *Science*, 239, 390-392, 1988.
- Conrad, S. H., J. L. Wilson, W. R. Mason, and W. J. Peplinski, Visualization of residual organic liquid trapped in aquifers, *Water Resour. Res.*, 28, 467-478, 1992.
- Derjaguin, B. V., and L. Landau, Theory of the stability of strongly charged lyophobic sols and of the adhesion of strongly charged particles in solutions of electrolytes, *Acta Physicochim. URSS*, 14, 633-662, 1941.
- Derjaguin, B. V., S. S. Dukhin, and N. N. Rulyov, Kinetic theory of the flotation of fine particles, *Surf. Colloid Sci.*, 13, 71-113, 1984.
- Derjaguin, B. V., N. V. Churave, and V. M. Muller, Surface forces, report, Consultants Bur., New York, 1987.
- Elimelech, M., and C. R. O'Melia, Effect of particle size on collision efficiency in the deposition of Brownian particles with electrostatic energy barriers, *Langmuir*, 6, 1153-1163, 1990.
- Fuerstenau, D. W., Fine particle flotation, in *Fine Particle Processing*, vol. 2, edited by P. Somasundaran, pp. 669-691, American Institute of Mining and Engineering, New York, 1980.
- Gaudin, A. M., A. F. Witt, and T. G. Decker, Contact angle hysteresis: Principles and application of measurement methods, *Trans. Am. Inst. Min. Metall. Pet. Eng.*, 226, 107-112, 1963.
- Gschwend, P. M., Colloids in groundwater: Their mobilization, subsurface transport, and sorption affinity for toxic chemicals, *Rep. DOE/ER/60846-3*, Subsurface Sci. Program, Office of Health and Environ. Res., Washington, D. C., 1992.
- Hamaker, H. C., The London-van der Waals attraction between spherical particles, *Physica*, 4, 1058-1072, 1937.
- Hirasaki, G. J., Wettability: Fundamentals and surfaces, *SPE Form. Eval.*, 1, 217-226, 1991.
- Hornaby, D., and J. Leja, Selective flotation and its surface chemical characteristics, *Surf. Colloid Sci.*, 12, 217-314, 1983.
- Israelachvili, J. N., *Intermolecular and Surface Forces*, Academic, San Diego, Calif., 1991.
- James, D. F., The meniscus on the outside of a small circular cylinder, *J. Fluid Mech.*, 63, 657-664, 1974.
- Jameson, G. J., Physical aspects of fine particle flotation, in *Principles of Mineral Flotation*, edited by M. H. Jones and J. T. Woodcock, pp. 215-236, Australia Institute of Mining and Metallurgy, Victoria, Queensland, 1985.
- Laskowski, J., Particle-bubble attachment in flotation, *Miner. Sci. Eng.*, 6(4), 223-235, 1974.
- Lee, C. Y., and J. A. McCammon, The structure of liquid water at an extended hydrophobic surface, *J. Chem. Phys.*, 80, 4448-4456, 1984.
- Leja, J., *Surface Chemistry of Froth Flotation*, Plenum, New York, 1982.
- Li, C., and P. Somasundaran, Reversal of bubble charge in multivalent inorganic salt solutions: Effect of magnesium, *J. Colloid Interface Sci.*, 146, 215-218, 1991.
- McCarthy, J. F., and J. M. Zachara, Subsurface transport of contaminants, *Environ. Sci. Technol.*, 23, 496-502, 1989.
- McDowell-Boyer, L. M., J. R. Hunt, and N. Sitar, Particle transport through porous media, *Water Resour. Res.*, 22, 1901-1921, 1986.
- Rapachietta, A. V., and A. W. Neumann, Force and free energy analysis at fluid interfaces, II, Spheres, *J. Colloid Interface Sci.*, 59, 555-567, 1977.
- Van Loosdrecht, M. C. M., J. Lyklema, W. Norde, G. Schraa, and A. J. B. Zehnder, Electrophoretic mobility and hydrophobicity as a measure to predict the initial steps of bacterial adhesion, *Appl. Environ. Microbiol.*, 53, 1898-1901, 1987.
- Van Oss, C. J., J. Visser, D. R. Absolom, S. N. Omenyi, and A. W. Neumann, The concept of negative Hamaker constant, *Adv. Colloid Interface Sci.*, 18, 133-148, 1983.
- Verwey, E. J. W., and J. T. G. Overbeek, *Theory of Stability of Lyophobic Colloids*, Elsevier, New York, 1948.
- Williams, D. F., and J. C. Berg, Aggregation of colloidal particles at the air-water interface, *J. Colloid Interface Sci.*, 152, 218-229, 1992.
- Wilson, J. L., S. H. Conrad, W. R. Mason, W. Peplinski, and E. Hagan, Laboratory investigation of residual liquid organics from spills, leaks, and the disposal of hazardous waters in groundwater, *Rep. EPA/600/690/004*, R. S. Kerr Environ. Res. Lab., Ada, Okla., 1990.
- Yoon, R. H., and J. L. Yordan, Zeta potential measurements on microbubbles generated using various surfactants, *J. Colloid Interface Sci.*, 113, 430-438, 1986.

J. Wan, Lawrence Berkeley Laboratory, Mail Stop 50E, 1 Cyclotron Road, Berkeley, CA 94720.

J. L. Wilson, Department of Geoscience, New Mexico Institute of Technology, Socorro, NM 87801.

(Received February 4, 1993; revised August 10, 1993; accepted August 24, 1993.)